Preprints (www.preprints.org) | NOT PEER-REVIEWED | Posted: 8 July 2019 doi:10.20944/preprints201907.0102.v1

Article

The Brain Origin of Neonatal Microglia Determines the Content of Exosomes and Biological Function

Adriana-Natalia Murgoci [1, 2, 3], Khalil Mallah [1], Soulaimane Aboulouard [1], Christophe Lefebvre [1], Milan Cizek [4], Isabelle Fournier [1], Dasa Cizkova [1, 2, 3,*] and Michel Salzet [1,*]

[1] Inserm, U-1192 - Laboratoire Protéomique, Réponse Inflammatoire et Spectrométrie de Masse-PRISM, Université Lille, 59650 Villeneuve d'Ascq, France
[2] Institute of Neuroimmunology, Slovak Academy of Sciences, Dúbravská cesta 9, Bratislava 845 10, Slovakia
[3] Department of Anatomy, Histology and Physiology, University of Veterinary Medicine and Pharmacy in Košice, Komenského 73, Košice 041 81, Slovakia
[4] Department of Epizootiology and Parasitology, University of Veterinary Medicine and Pharmacy in Košice, Komenského 73, Košice 041 81, Slovakia
* Correspondence: michel.salzet@univ-lille1; Tel.: +33 (0)3 20 43 41 94 (M.S.), dasa.cizkova@uvlf.sk; Tel.: +421 2 5478 8100 (D.C.).

Abstract: Using a combination of pan proteomic platform associated with systemic biology analyses, we demonstrate that neonatal microglial cells derived from cortex and spinal cord expressed different phenotypes upon the physiological or pathological conditions. They also highlight great variability in protein production on both cellular and exosome levels. Bioinformatics data indicate for the cortical microglia anti-inflammatory and neurogenesis/tumorigenesis characteristics, while for the spinal cord microglia involvement in the inflammatory response. We confirmed these results by performing functional testing including neurite outgrowth assays in DRGs cell line, and glioma proliferation analysis in 3D spheroid cultures. Results from these in vitro assays indicate that the microglia located at different CNS areas reveal differential biological functions. While both microglia sources enhanced growth of DRGs axons, only the spinal microglia significantly attenuated glioma proliferation. Overall these findings are pointing to the fact that the origin of neonatal microglia affects the physio-pathological function, which may address the prevalence of the glioma in the brain in comparison with the spinal cord in adult.

Keywords: Microglia exosomes; 3D culture; Proteomic study

1. Introduction

Myeloid cells residing in the central nervous system (CNS) are key players of the crosstalk that is continuously established between the nervous and immune systems. Recent studies have shown that the CNS hosts diverse populations of myeloid cells that include parenchymal microglia, macrophages and dendritic cells that are settled in the leptomeninges, perivascular space and choroid plexus [1–3]. Experimental studies involving novel transgenic mouse models have clearly shown that unlike brain cell types of neuroectodermal origin, microglia and their non-parenchymal counterparts originate exclusively from prenatal hematopoietic stem cells (HSCs) of yolk sac at E7.5-E8, before the blood brain barrier is established [1–7]. In course of neurodevelopment, neurons and glial cells crosstalk lead to formation of microglia structure performing specific function within the mature neuroimmune system [8–15].

Among the glial cells, microglia represent 5-10% of the total CNS cells [3,16]. They migrate into the early brain at stage E9.5 and become resident cells through life [5,16]. Recently the role of microglia has been investigated in the process of cerebellum development. The work of McCarthy

© 2019 by the author(s). Distributed under a Creative Commons CC BY license.

Preprints (www.preprints.org) | NOT PEER-REVIEWED | Posted: 8 July 2019 doi:10.20944/preprints201907.0102.v1

group has demonstrated a continuous process of microglial maturation and a non-uniform distribution of microglia in the cerebellar cortex [17].

In this context it is important to understand whether microglia cells migrating in other CNS components, in the neocortex or in the spinal cord, are subjected to the same maturation processes and share similar functional phenotypes. Furthermore, most of the parenchymal microglia and their counterparts-macrophages receive no contribution from the bone marrow or liver progenitors, which further indicates the importance of the surrounding environment in specific anatomical CNS areas during development and adulthood [5,18–23]. Despite this fact, these immunocompetent and phagocytic cell populations at the CNS interfaces represent long-lived cells with a considerable self-renewal capacity [24].

As in the brain, the spinal cord microglial cells infiltrate the embryonic parenchyma through the peripheral vasculature and are gradually aggregated in the dorsolateral, ventral regions, and in the lateral motor columns and finally are randomly distributed within the parenchyma [16]. Indeed, all these myeloid populations exhibit an intimate relationship within the CNS, where they support tissue homeostasis during neuronal development, synaptic remodeling and have important pathophysiological roles in adulthood immune and neuronal functions [7,16].

CNS myeloid cells are classified according to their distinct anatomical localization, morphological features and surface-marker expression such as Iba-1, F4/80, CD11b and the fractalkine receptor CX3CR1 [23,25]. Microglial cells comprise a characteristic molecular content, defined as a bio-molecular signature, which is transferred from one cell to another via extracellular vesicles (EVs) as exosomes [26,27]. Microglia exosomes play an important role in communication with neurons and other glial cells including astrocytes and oligodendroglia cells [28]. Based on recent studies, it is believed that by engineering microglia cells, it will be possible to modulate derived vesicles and redirect microglia towards a neuroprotective phenotype, promoting beneficial effects in neurodegenerative diseases associated with neuroinflammatory processes [9,15,29,30]. However, to initiate microglial-derived exosome-based drug delivery system, it is important to develop fundamental neurobiological knowledge by exploring exosomes and their cargo, which is distributed within different brain and spinal cord regions.

Today we know that there are differences between the genes expressed by microglia during different developmental stages of the brain and that environmental factors have a strong influence on the growth and function of microglia [31,32]. These findings suggest that microglia heterogeneity correlate with: i) spatial distribution of microglia in different regions of the adult brain, ii) temporal condition of microglia during different developmental stages and iii) pathological conditions that modify microglia [31–35].

In present study, we focused on neonatal microglia isolated from rat pups 3-4 days old. Here, we have investigated through proteomic and biological essays the influence of the anatomical spatial localization of the isolated microglia i.e. cortex versus spinal cord microglia on the nature of their secreted exosomes under resting condition and pro-inflammatory stimulation.

2. Materials and Methods

2.1. Chemicals

All chemicals used were purchased with the highest purity available. The formic acid (FA), trifluoroacetic acid (TFA), acetonitrile (ACN), methanol (MeOH) and water were obtained from Biosolve B.V. (Valkenswaard, Netherlands). From Sigma (Saint-Quentin Fallavier, France) were obtained the thiourea, DL-dithiothreitol (DTT) and iodoacetamide (IAA). The Trypsin/Lys-C Mix, Mass Spec Grade was obtained from Promega (Charbonnieres, France).

2.2. Experimental Design and Statistical rational

All experiments were conducted with biological replicates (n=3). A total of 12 rat were included in the study for isolations of spinal cord and cortex microglia exosomes, treated or not with

Preprints (www.preprints.org) | NOT PEER-REVIEWED | Posted: 8 July 2019 doi:10.20944/preprints201907.0102.v1

lipopolysaccharides. The statistical analysis carried out for these microglia cultivated in presence of LPS or not was multiple sample ANOVA test with a p-value=0.01. Proteomic preformed on Microglia and exosomes analyses, Student's T-test was applied with a p-value= 0.05. Normalization was achieved by using the Z-score. Data analysis was carried out on Perseus Software.

2.3. *Animals*

All animal studies were performed with approval of the Institutional Animal Care and Use Committee of the SAS, and in line with the guidelines of the European Communities Council Directive (2010/63/EU), Slovak Law for Animal Protection No. 377/2012, 436/2012 and animal protocol approval Ro-4081/17-221.

2.4. *Cells and culture conditions*

Primary microglia cultures. Primary microglia cells were isolated according to our previously published procedure [36]. Briefly neural stem cells (NSCs) were dissociated from cortex and spinal cord of Wistar rat pups (P3), by Papain Dissociation System (Worthington Biochem. Corp., NJ, USA). Using CD11b/c (Microglia) MicroBeads (Miltenyi Biotec Inc., CA, USA) in conformity with the manufacturer's instructions microglia cells were separated from cell suspension. The isolated microglia were cultured in Dulbecco's Modified Eagle Medium/Ham's Nutrient Mixture F-12 (DMEM/F12, 1:1) (BIO SERA, BioTech, Bratislava, SK) supplemented with 10% of fetal bovine serum (FBS) (GE Healthcare, Biowest, South America), 0.1% antibiotics (gentamicin 50mg/mL, Sigma-Aldrich), 1% ultraglutamine (200mM, Lonza), 10% B27 Supplement (Gibco), 10% N2 Supplement (Gibco). The cells were plated for 7 days in cell culture plates pre-coated with poly-L-lysine 50µg/mL (Sigma), incubated in a humidified atmosphere with 5% CO2, 37°C.

Efficacy of microglia separation: immunocytochemistry analyses. Cells fixation was made with paraformaldehyde (PFA) 4% for 10 min at 37°C. For blocking was used 5% BSA and 0.1% Triton X PBS, for 60 min at room temperature (RT), then the cells were washed 3 times and incubated O/N with primary antibody anti-Iba1 (1:500, rabbit polyclonal antibody; Wako Pure Chemical Industries, Osaka, Japan) concurrent with anti-GFAP (1/200, mouse monoclonal antibody, ab 10062 , Abcam) both diluted in PBS with 5% BSA and 0.1% Triton. Next day the slides were washed 3 times and incubated with the secondary fluorescent antibodies, Alexa Fluor 488 goat anti-rabbit IgG (, Invitrogen) and Alexa Fluor 546 goat anti-mouse IgG (Invitrogen), both diluted 1/2000 in PBS with 5%BSA and 0.1% Triton, for 2h, at RT, in the dark. The slides were mounted using Fluoroshield medium with DAPI (Sigma). Labelled cells were analyzed with fluorescence microscope Zeiss LSM710. The microscope pictures were processed with Zen10 software (Zeiss).

2.5. *Microglia derived exosomes isolation*

Confluent primary microglia culture (≈5x10^5 cells) at 7 days was supplemented with FCS free DMEM containing 500 ng/mL lipopolysaccharide (LPS, Invivogen, Toulouse, FR) or not for 24h. Afterwards conditioned medium was removed and was cleared of debris using centrifugation steps 350 × g, 10 min at 4°C and filtration by 0.20 µm filter. The method of exosomes isolation assumes differential steps of centrifugation and ultracentrifugation. By centrifugation for 30 min, 2,000 × g at 4°C, the membranes and debris were removed and obtained cleared medium. Next step was centrifugation at 10000 × g, 30 min, at 4°C to remove ectosomes and larger vesicles. To obtain exosomes pellet, the supernatant was ultracentrifuged (Beckman Optima TLX Ultracentrifuge, USA) at 100000 × g for 70 min, 4°C. To eliminate contaminating proteins, the exosomes pellet was washed with 10 ml PBS and re-ultracentrifuged at 100000 × g for 120 min, 4°C. The exosomes pellet was stored at -20°C.

Preprints (www.preprints.org) | NOT PEER-REVIEWED | Posted: 8 July 2019 doi:10.20944/preprints201907.0102.v1

2.6. Nanoparticle tracking analysis (NTA)

Isolated vesicles were analyzed using NanoSight LM 10 instrument (Merkel technologies LTD., UK) to characterize the size and concentration. After last ultracentrifugation step, the pellet obtained was diluted in particle-free PBS (1:100). To analyze the particles, 5 videos of 60 s for each sample were recorded. A monochromatic laser beam at 488nm was used for analyses. Particle movement was investigated with NTA software (version 3.2, NanoSight). NTA post-acquisition settings were kept constant between samples. Each sample was analyzed in triplicate (n=3).

2.7. Functional analyses of microglia exosomes

ND7/23 cell line (Sigma, neural / neuroblastoma, hybrid rat / mouse, DRG) have been utilized to analyze the neurite outgrowth in vitro influenced by exosomes released by cortex microglia or spinal cord microglia cells. DRGs cells were cultivated 50 000 cells/per well, 12h before treatment in DMEM medium enrich with 2% fetal bovine serum (FBS) + 1% antibiotics (10,000 units/mL penicillin, 10,000 µg/mL streptomycin, Invitrogen, Thermo Fisher Scientific) + 1% L-Glutamine (Sigma). Afterwards, cells were treated with microglia exosomes (1,5x108 particles/ml) or with microglia conditioned medium for 24h and 48h. The measurements for neurites outgrow were performed by using ImageJ software. For statistical significance evaluation the One-Way ANOVA by GraphPadPRISM software was applied.

C6 rat glioma cells were used to form 3D glioma spheroids [37,38]. In brief C6 cells were resuspended in cDMEM to obtain 12500 cells in 200 µl. 200 µl of cell suspension was distributed in drops on low attachment surface plates which was incubated at 5% CO2, 37°C for 96h to form the cell spheroids. Once formed, the spheroids were transferred to a 24-well plate, one spheroid per well in 400 µl of 2.2 mg/ml collagen mixture as we described in previous publication [38].

2.8. Microglia cells: proteins isolation and identification

Protein extraction was performed by adding 50 µl of extraction buffer (4% SDS, Tris 0.1M, pH 7.8) to each sample. After mixing well, the samples were heated at 95 °C for 15 min followed by a sonication step of 15 min. Samples were then centrifuged at 16,000 g for 10 min at 20 °C. Finally, the supernatant (containing extracted proteins) was collected. Following the extraction process, all protein samples were quantified using Bradford quantification method and concentration of samples was normalized.

2.9. Filter-aided sample preparation (FASP)

For protein processing, a shotgun bottom-up approach was applied. 30 µl volume of each sample was prepared after the normalization in the previous step, to obtain a final concentration of 1.5 µg/µl per sample. An equal volume of reduction solution (DTT 0.1 M) was added to each sample then incubated 40 min at 56 °C. Using FASP method [39] the samples were processed. This technique utilizes a filter with a nominal molecular weight limit of 30,000 (Amicon Ultra-0.5 30k, Millipore). After transferring the samples into the FASP filters, alkylation step was done using IAA solution (0.05 M) for 20 min in the dark at room temperature. Digestion was then carried overnight at an incubation temperature of 37°C using LysC/trypsin (40 µg/ml in 50 mM Tris-HCL solution at pH 8). The filters containing the digests were then rinsed using 50 µl of saline solution (0.5 M) and the enzyme activity was stopped with 10 µl of TFA 5% for each tube. Enrichment and desalting were then performed for each sample with a ZipTip C-18 (Millipore) before undergoing LC-MS/MS analysis.

2.10. MS data acquisition

Preprints (www.preprints.org) | NOT PEER-REVIEWED | Posted: 8 July 2019 doi:10.20944/preprints201907.0102.v1

The analyses were carried out by an Easy-nLC 1000 nano-UPLC chromatography (Thermo Scientific) interfaced with a Q-Exactive Orbitrap mass spectrometer (Thermo Scientific) with a nano-electrospray ion source. The analysis was performed in reverse phase and the sample was loaded into a pre-concentration column (75 µm DI × 2 cm, 3 µm, Thermo Scientific). Using an analytical column (Acclaim PepMap C18, 75 µm ID × 50 cm , 2 µm, Thermo Scientific) by applying a linear gradient of acetonitrile in 0.1% formic acid (5% to 35%, for 2 hours) at 300 nL/min flow rate the peptides were separated. MS analysis was performed by Orbitrap mass analyzer with a resolution of 70,000 FWHM, a mass range of m/z 300-1600, an AGC of 3e6 ions and a maximum injection time of 120 ms. The MS/MS was performed in dependent data mode, defined to analyze the 10 most intense ions of MS analysis (Top 10). For MS/MS parameters, the resolution is set to 17,500 FWHM, a mass range of 200-2000 m/z, an AGC of 5e4 ions, and a maximum injection time of 60 ms. The isolation window is set at 4.0 m/z.

2.11. Data processing

All data were analyzed by MaxQuant software version 1.5.8.3 [39]. Proteins were identified by comparing all the spectra with the proteome reference database of Rattus norvegicus (Uniprot, release April 2017, 7983 entries). The digestion enzyme used was LysC/trypsin and the maximum of missed cleavages allowed was two, in addition to oxidation of methionine and N-terminal protein acetylation selected as variable modifications. Carbamidomethylation of cysteine was selected as fixed modifications. For protein identification, a minimum of 2 peptides of which 1 was unique was defined. In MS mode, an initial mass tolerance of 6 ppm was selected, and the MS/MS tolerance was set to 20 ppm for fragmentation data. The false discovery rate (FDR) was specified to 0.01 for protein and peptide. The label-free quantification (LFQ) has been realized with keeping the default parameters of MaxQuant. The statistical analysis of identified proteins was performed by Perseus software version 1.5.2.6. The matrix was filtered by removing the potential contaminant, reverse and only identified by site. Then, the samples were grouped into 4 categories: Cortex Control, Cortex LPS, Spinal Cord Control, and Spinal Cord LPS. Statistical analysis was performed by ANOVA test with a p-value of 5%. Hierarchical clustering and profile plot were performed and visualized by Perseus.

2.12. Microglia derived exosomes: protein isolation and identification

Microglia exosomes proteins were extracted with RIPA buffer and prepared for LC MS/MS analysis using FASP protocol previously described. For MS data acquisition were used the same instruments and methods as for microglia proteins.

Using MaxQuant (version 1.5.1.2) with Andromeda search engine, all MS data obtained were analyzed. The proteins were identified by comparing all the spectra with the proteome reference database of Rattus norvegicus (Uniprot, published in June 2014, with 33,675 entries), merged with commonly detected 262 contaminants [40–42]. The same digestion enzyme used for exosomes samples, so for protein identification the same methods as for microglia proteins were applied.

3. Results

3.1. Different origins of microglia do not accuse morphological differences between cells

Neural stem cells (NSCs) were isolated from rat pups postnatal day 3 or 4 (P3/4) (n=10) using Papain Dissociation System (**Supp. data 1A**). Microglia cells, positive for CD11 b/c antibody, were separated from other NSCs (astrocytes, oligodendrocytes, neurons, fibroblasts) using CD11b/c MicroBeads [36], obtaining 10.10% microglia cells for spinal cord and 11.88% microglia cells for cortex (**Supp. data 1B**). The immunocytochemistry using primary antibody anti-Iba1 and anti-GFAP confirmed that CD11b/c MicroBeads procedure had a good efficacy for obtaining more than 90%

Preprints (www.preprints.org) | NOT PEER-REVIEWED | Posted: 8 July 2019 doi:10.20944/preprints201907.0102.v1

microglia cells (**Figure 1** and **Supp. data 1C and 1D**). Untreated microglia cells revealed a filament shape morphology with long branches (**Figure 1A and 1C**). The incubation with 500 ng/mL LPS for 24h induced persistent activation of microglia with the morphological changes (**Figure 1B and 1D**). Cells retract their processes and exhibit an occasionally ramified structure of amoeboid shape (**Figure 1B and 1D**). However, there were no morphological differences between cortex and spinal cord microglia cells under control conditions or subjected to LPS treatment, comparing Figures 1A with 1C, and 1B with 1D.

3.2. Proteomic studies established a territory profile of the microglial cells

Microglia isolated from cortex or spinal cord treated or not with LPS were subjected to protein extraction followed by shotgun proteomic analyses. We have identified 2082 significant grouped proteins (**Supp. data 2**) with 295 identified proteins from cortex microglia (21 unique for control, 115 unique for LPS treated cells and 159 common for both conditions) and 111 from spinal cord microglia (19 unique for control, 90 unique for LPS treated cells and 2 common for both conditions) (**Figure 2A**).

3.2.2. Cortex microglia

Pathway analyses based on the identified proteins revealed that microglia derived from the cortex are more involved in neuronal migration, exogenesis and monocytes recruitment under physiological untreated condition. Between specific proteins identified are Mark2, Alcam and Rhob. By contrast, after LPS stimulation, the protein pathways by taking care the highest p-value correspond to cell proliferation and growth (**Figure 2B**). The specific proteins identified are presented in **Table 1**.

3.2.2. Spinal cord microglia

In microglia derived from the control spinal cord, pathways showed that proteins are mostly involved in Na+/H+ antiporter nerve degeneration and lipid degradation corresponding to Nr3c1, Gnat3, and Lipa proteins (**Table 1)**. In LPS treated spinal cord microglia, the proteome profile highlight pathways that are more devoted to inflammation including complement pathways and macrophages activations, corresponding to Cd59, Cd200rl or Cdk9 proteins, and cell proliferation (**Figure 2C** and **Table 1)**. Common pathways between spinal cord microglia under control and LPS treatment are linked to hyperalgesia after injury. In contrast, the common ones found with cortex microglia cells are related to cancer and cell differentiation (**Table 1** and **Supp. data 3**).

To better understand the modulation registered in relation to two different sources of microglia and the impact of the LPS treatment, ANOVA tests were performed with non-supervised clustering of samples. Two main clusters were highlighted. First cluster represents overexpressed proteins in both cortex and spinal cord after LPS stimulation, while second cluster groups overexpressed proteins only in cortex microglia cells (**Figure 2D** and **Table 2)**. A single protein has been found overexpressed solely in spinal cord in control, the UPF0183 protein C16orf70 homolog which is known to bind on glutamate receptor. Pathways for each cluster have been realized based on systemic biology analyses (**Figures 2Db, 2Dc** and **Table 2)**. Cluster 1 presents proteins involved in inflammation and adaptive immune response (**Figure 2Db**) whereas, cluster 2 present proteins which are more devoted to neuroblastoma and cancer processes (**Figure 2Dc**). All these proteins are under-expressed in microglia from spinal cord. We focused our interest on the proteins involved in inflammation and neurogenesis (**Table 3**). Label-free quantification value clearly revealed that proteins involved in inflammation-like processes (caspases, NLRC4, interleukin 18) are over-expressed in microglia from cortex stimulated by LPS, whereas IL1β is major cytokine found in the control cortex microglial cells. Only a few proteins involved in inflammation are overexpressed significantly in spinal cord microglia treated with LPS (IL1β , Mepg1, MX1, MX2, CCL7, Capg, Mpcg1, Aim, Caspase 8, Plec). Analysis of immune protein receptors such as CD4, CD36, CD38,

Preprints (www.preprints.org) | NOT PEER-REVIEWED | Posted: 8 July 2019 doi:10.20944/preprints201907.0102.v1

CD48, was shown to be overexpressed in cortex microglia after LPS treatment, whereas the neonatal Fc receptor subunit 51 was shown to be decreasing in cortex microglia after LPS stimulation (**Table 3**). Low antibodies affinity receptors (CD16, CD32) increased in LPS stimulated cortex microglia and regulated in the ones from spinal cord microglia.

It is worth noting that CD4, CD44, CD48, are not detected or quantitatively decreased in spinal cord microglia whereas they are over-expressed in cortex microglia after LPS stimulation. Several factors involved in inflammation regulation have been identified in microglia from spinal cord. For example, CD59, CD63 and CD200 are only detected or quantitatively increased in microglia issued from spinal cord. CD200 is known to modulate spinal cord injury neuroinflammation [43]. CD59 is modulating complement response, CD63 is a marker of exosomes. Osteoclast-stimulating factor-1 (Ostf1) has been detected in microglia from spinal cord and absent from the ones issued from cortex whereas the secreted phosphoprotein 1 (Ssp1) is only found in cortex microglia. These two proteins are known to be involved in neurogenesis processes [15,44].

3.3. Proteomic analyses of exosomes released by microglia cells

Isolation procedure of microglia derived exosomes was performed using serial centrifugations (**Supp. Figure1**). Quality control was performed by NanoSight quantification. Exosomes derived from cortex microglia are more homogenous to the ones from spinal cord (**Supp. data 4**).

Proteomic studies confirm also differences between the naturally occurring proteins identified in the microglial exosomes derived from different source (**Figure 3**). Microglia exosomes have been subjected to shotgun proteomic analyses and 382 proteins have been identified in total (**Supp. data 5-8**). 116 proteins were shown to be identified exclusive to the exosomes derived from cortex microglia and 28 proteins were identified specific for exosomes derived from spinal cord microglia. 34 proteins were specific for exosomes of control microglia and 76 proteins were specific for exosomes of microglia treated with LPS, while 50 proteins correspond for exosomes derived from control spinal cord microglia and 52 proteins for exosomes derived from spinal cord microglia treated with LPS (**Figure 3A**).

According to Exocarta database (http://exocarta.org/) and EVpedia [45], we identified in both microglial sources (cortex and spinal cord) proteins which are considered markers for exosomes e.g. CD9, CD81, Annexin (**Supp. data 9**) and for microglia (**Supp. data 10**). Identified protein Lgals1 (axonal growth promoter) associated with Gpnmb (neuroprotective factor), Gpx1 (promotor of neurites outgrowth) with Vim, Fabp5 and Spp1 (implicated in neurodevelopment process), are markers of neonatal microglia [15]. The proteome network reveal proteins involved in neurite outgrowth, nerve regeneration and axonogenesis (**Figures 3B and 3C**). By contrasts, pathways associated with spinal cord microglia's exosomes shows correlation to inflammation and injuries (**Figure 3D**). Global analyses of exclusives exosomes proteins from the two microglia sources highlight this dichotomy i.e. inflammation (spinal cord origin) vs. nerve regeneration (cortex origin) (**Figure 3E**).

A further study of exosomal proteome quantitative assessment showing significant abundance among the samples was computated using the MaxQuant software and Perseus operating system. As a criterion of significance was applied ANOVA test with significance threshold of $P<0.05$. After statistical analyses heat maps were engendered (**Figure 3F and Supp. data 11-14**). Heat map presents two main branches i.e. one for cortex under LPS stimulation and the second one is related to spinal cord and control cortex. This branch is then subdivided between spinal cord and control cortex. From these data, three over-expressed clusters could be retrieved **(Figure 3F**). Enriched pathways have been analyzed from the significantly abundant proteins present in each cluster (**Figure 3F**). Cluster 1 contains 57 proteins which is related to the ones isolated from spinal cord. It is subdivided in two branches which separates control and LPS treated microglia. Some of identified proteins are involved in inflammation (Cfh, mrc2, C4a, Lgal3bp, Lgals1, C1S, and Cfhr1) or in neurogenesis (Spp1, Spon1, Sned1, Srpx, Hspg2, Fstl1, and Olfml3) (**Supp. Data 10**). In cluster 2, corresponding to the LPS-treated cortex microglia, proteins are mostly involved in chemotaxis, NFkB pathway and present in glioma. Several of the identified proteins are implicated in metabolic

Preprints (www.preprints.org) | NOT PEER-REVIEWED | Posted: 8 July 2019 doi:10.20944/preprints201907.0102.v1

processes. Importantly, 27 of the 136 of the proteins have already been reported as markers of exosomes, such as Hist1h1b or HSP90ab1 (**Supp. Data 10**). The last cluster, which is specific to control cortex microglia, is highly connected to neurodegenerative diseases or autoimmune diseases. It contains 35 proteins and between them we detected markers of exosomes, such as CD9, Mug2 Actn4 or Gdl2 (**Supp. Data 9-10**). Among the proteins identified in cluster 3, some are known to be involved in neurites outgrowth modulation (CspG4, Bcan, ApoE, Sparcl1, Chadl) and others are associated with glioma proliferation (Cd9, Igfbp2, Hyou1, Ldhb, LdhA, LdhC, Acly, Calu).

3.4. Biological activities of microglia exosomes

To confirm such differences between the microglia exosomes derived from the two anatomical regions (cortex or spinal cord), several biochemical and functional biological tests were conducted. The first test performed compared the impact of exosomes vs condition medium (CM) derived from cortex or spinal cord microglial cells on dorsal root ganglion (DRG) neurites outgrowth (**Figure 4**). Exosomes or the CM were added to the DRG culture medium similarly as in previous studies [46–48]. The percentage of neurites emergence was measured 24h, 48h and 72h after exosomes or CM incubation. As presented in **Figure 4A**, exosomes derived from both microglia sources under control or LPS conditions significantly stimulated neurite outgrowth already at 24h when compared to DMEM control. However, a difference was registered between the microglia source i.e. cortex exosomes enhanced 60-70%, while spinal cord exosomes 80-85% of DRG neurites (**Figure 4A**). At 48h, the results slightly progressed, while at 72h decreased, although significant differences on neurite growth between cortex and spinal cord microglia exosomes remained. Similar results were registered when considered the neurites length, where cortex and spinal cord microglial exosomes stimulated neurite outgrowth within range of 60µm-90µm, and 50µm-65µm respectively (**Figure 4C**). Surprisingly, the longest neurites were documented after incubation with exosomes derived from control cortex microglia (60µm -150 µm). Moreover, LPS treatment in general reduced the length of the neurites compared to the control (Figures 4C). This can be explained by the presence of pro-inflammatory chemokines (CXCL1, CXCL2, CXCL3, CCl2, CCL7) and IL6, TNF-alpha in LPS stimulated microglia. Second set of experiments showed that, conditioned medium had similar effect as exosomes, in terms of percentage of neurites emergence and neurites length at 24h. The real differences between microglia exosomes and microglia's conditioned medium on neurite outgrowth occurred at 48h and 72h, when the % of neurites dropped for exosomes to 40% compared to 70% with CM (**Figure 4B**). Taken together, these biological effects are partially in line with the enriched pathway reflecting the ability of exosomes to stimulate neurites outgrowth (from cortex microglia) and inflammation (from spinal cord microglia). In this biological test, time course is a key player. Exosomes could stimulate neurites outgrowth, with the highest activity for the ones derived from spinal cord exosomes at 24h and 48h.

The second biological essay was based on glioma proliferation using 3D spheroids cultures as published in previous studies [37,38]. In these conditions, the exosomes were placed in contact with 3D glioma C6 spheroids and a time course proliferation or inhibition was studied until 6 days (**Figure 5A**). In this context, the highest anti-proliferative effect was observed at 24h and 48h with exosomes released from LPS treated spinal cord microglia (Figure 5B). Around 50% inhibition was detected by these exosomes. In contrast, the exosomes derived from the cortex microglia as reflected by the enriched pathways, stimulate glioma proliferation (**Figure 5**).

4. Discussion

Authors should discuss the results and how they can be interpreted in perspective of previous studies and of the working hypotheses. The findings and their implications should be discussed in the broadest context possible. Future research directions may also be highlighted.

Microglia possesses distinctive ontogeny and morphology compared to other glial and neural cells [49]. Those brain resident macrophages are important sentinels constituting the first line of

Preprints (www.preprints.org) | NOT PEER-REVIEWED | Posted: 8 July 2019 doi:10.20944/preprints201907.0102.v1

response to injury, infection or inflammatory processes. They strongly interact with other brain cells regulating neural circuits and synaptic transmission [3,50].

As described recently, it is well established that tissue environment represents an important determinant of microglia identity. Present proteomic data confirmed differences in the proteome between microglia derived from cortex and spinal cord under physiological condition and following LPS stimulation. Identified proteins and corresponding pathways suggest that resting cortex microglia are important for neurogenesis, while stimulated microglia may contribute to cell proliferation and growth. These results are in line with findings in mouse and human brain, demonstrating high proliferative activity of short-lived microglia, but also variations in proliferation and apoptosis across different brain regions [51]. Interestingly, human microglia in the subventricular zone and thalamus showed higher expression of proliferative markers (Ki-67, cyclin A, B) compared with other brain regions [52]. Whether increased proliferation pattern within the brain specific regions correlates with tumorogenity remains to be investigated. On the contrary, the control spinal cord proteome and corresponding pathways seems to be associated with the nerve and lipid degenerative processes, while under stimulation they are linked to inflammation including complement pathways. It is well documented that pro-inflammatory processes in the brain lead to neurodegenerative changes and cognitive decline. The neuroinflammation is a broad process in terms of the activation of microglia, which are nowadays viewed as heterogeneous resident immune cells [52]. Although microglia functions are still unclear in amyotrophic lateral sclerosis (ALS), a recent study described that tissue-specific microglia can be a pathological hallmark of ALS [53]. Indeed, stronger pro-inflammatory responses were measured in wild-type spinal versus cortical microglia, suggesting that spinal microglia are more reactive in ALS, which is also in line with our proteomic and bioinformatics data. These results are in line with our data. Here, we have shown that neonatal microglia derived from different anatomical CNS regions have an anatomical territory-specific phenotype i.e. cortex microglia play a key role in neuronal migration and exogenesis while spinal cord microglia in inflammatory processes [54]. Thus, the tissue microenvironment during development can contribute to a microglia specific molecular pattern within distinct CNS regions. It is now accepted that microglia in cortex are derived from the yolk sac macrophages which are seeding the brain rudiment during early fetal development [55]. On the other hand, the microglia cells present in spinal cord are still controversial as to their contributing role origin and function [3,7].

In fact, exosomes released from cortex microglia possess markers (Olfml3, Hexb (instead Hexa), Fabp5, Cspg4, Fam3, Lgals1) which allow establishing their cellular origin [4,15,25]. Moreover, these exosomes reveal their neonatal nature by presenting neuroectodermal markers (Spp1, Lgals1, Gpx1) [15] associated with other proteins involved in brain development such as metalloproteases (Mmp2 and Mmp9), which are required for tissue remodeling [56], C1q and C3 needed for pruning axons, CCL2 and CCL7 involved in midbrain dopaminergic neurons differentiation [57]. The presence of the protein NOV homolog (CCN3) is also important since it plays a role in various cellular processes including proliferation, adhesion, migration, differentiation and survival. Furthermore, the matrix cellular protein CCN (CYR61/CTGF/NOV) is a member of large family including SPARC (secreted protein acidic and rich in cysteine), Hevin/SC1 (SPARC-like 1), TN-C (Tenascin C), TSP (Thrombospondin), which are secreted by astrocytes during development [58,59] and are also implicated in tumorigenesis [53]. These factors have a spatio-temporal expression in course of brain development (Supp. data 15). By contrasts, pathways associated with spinal cord microglia's exosomes shows correlation to inflammatory processes which correlate also with the cellular–based proteome of spinal microglia detected in present study. In addition, proteins identified (Cfh, GPR77, C4a, Lgal3bp, Lgals1, C1S, and Cfhr1) in spinal cord microglia exosomes are also produced by bone marrow-derived monocytes/macrophages [46,60] reinforcing the hypothesis of a different origin of the spinal cord microglia than the one present in brain. Furthermore, the functional biological tests with DRGs cell lines showed that, both exosomes and conditioned medium derived from microglia stimulate neurites outgrowth, with slight variations. These data are in line with other studies

Preprints (www.preprints.org) | NOT PEER-REVIEWED | Posted: 8 July 2019 doi:10.20944/preprints201907.0102.v1

documenting that altered microglia-derived exosomes (miR-124-3p) promoted neurite outgrowth after scratch injury or in vivo following brain trauma [61,62].

On the other hand, in glioma proliferation study using 3D spheroids cultures we have identified opposed microglia behavior, while the spinal microglia-derived exosomes revealed anti-proliferative effect, the cortex microglia-derived exosomes stimulate glioma growth. The presence of TNF-alpha and IL6 in LPS stimulated cortex microglia associated with metalloproteases (Mmp2, Mmp9) can drive the proliferation instead of inhibition [63,64]. Moreover, presence of SPARC, thrombospondin 1, tenascin C, osteopontin, Thrombospondin 2 and tensascin X seeds the tumor microenvironment [65]. Furthermore, in cortex microglia over-expression of CD44 and CD63 occurred, which are known to be involved in tumor metastasis, whereas they were absent in spinal cord microglia. This can also sustain the tumor proliferation inhibition registered with the exosomes isolated from LPS stimulated spinal cord microglia.

5. Conclusions

Taken together, these results established that exosomes produced by two different sources of microglia do not have the same pattern nor the same biological functions. Thus, microglia function is dependent on its cellular microenvironment which conditions its phenotype. In context of pathology such as glioma, this microglia phenotype can explain some territory tumor proliferation preference in one region compared to another one. Our results may indicate why glioma is more prevalent in brain than in spinal cord regarding the biological activity of the microglia obtained from different anatomical areas of CNS. Such hypothesis needs to be more deeply investigated, taking into consideration the best treatment in relation to the tumor localization as well as microglia expression pattern.

Supplementary Materials: The following are available online at www.mdpi.com/xxx/s1.

Author Contributions: Conceptualization, M.S. and D.C.; methodology, A.N.M.; software, A.N.M., F.K., S.A., K.M.; writing—original draft preparation, A.N.M., D.C., M.S., C.L., K.M., F.K., M.C.; writing—review and editing, A.N.M., D.C., M.S.; funding acquisition, M.S., D.C. and I.F.; All author reviewed, read and approved the manuscript.

Funding: This research was funded by INSERM, SIRIC ONCOLille Grant from DGOS-Inserm 6041aa (IF) and University Lille (ANM), APVV 15-0613 (DC), Stefanik SK-FR-2015-0018 (DC, MS), ERANET Axon Repair (DC).

Conflicts of Interest: The authors declare no conflict of interest.

The authors have declared no competing financial interests in this work.

Data and software availability: Spatially-resolved microproteomics, datasets including MaxQuant files and annotated MS/MS datasets, were uploaded to ProteomeXchange Consortium via the PRIDE database, and was assigned the dataset identifier.

Preprints (www.preprints.org) | NOT PEER-REVIEWED | Posted: 8 July 2019 doi:10.20944/preprints201907.0102.v1

Appendix A.1: Tables

Table 1. List of microglia cell proteins identified in function of tissue origin.

Tissue origin	Cell type	Identified proteins
Cortex	Microglia cells untreated	Mark2, Alcam, Micu2, Itgad, Lpl, Rhob
Cortex	Microglia cells treated with LPS 24h	Itpr2, Atp6ap2, Acaca, Amacr, Gch1, Pdk1, Cebpb, Ybx3, Ptpre, Clec2d, Ctcf, Cc2d1a, Tsc22d1, Nf2, Mapre2, Tubg1, Rad50, Cul7, Stx18, Kdelr1, Vamp2, Exosc9, Dmd, Sh2b2, Stk17b, Prpf4b, Rps27, Angptl4, Spp1, Jak2, Pak1, Taok1, Lyn, Daxx, Il18, Nek6, Aak1, Ptpra, Ppp1r14b, Ptpn2, Rab27b, Ctsh, Vmp1, Nlrc4, Adar, Pros1, Unc13d, Brcc3, Aldh1a2, Arfgap3, Elac2, Rbm3, Unc119, Crabp1, Sigmar1, Yipf3, Pggt1b, Fip1l1, Sh3glb2
Spinal cord	Microglia cells untreated	Nr3c1, F2, Gnb3, Ppp2cb, Gnat3, Gap43, Lipa
Spinal cord	Microglia cells treated with LPS24h	Cd59, Col2a1, Cr1l, Serping1, Dgat1, Hdac3, Khdrbs3, Kng1, Rgs10, Cd200r1, Sdc4, Htt, Lum, Ggt1, Kng1, Tollip, Mapk13, Camk2a, Cdk9, Cr1l, Inpp4a

Preprints (www.preprints.org) | NOT PEER-REVIEWED | Posted: 8 July 2019 doi:10.20944/preprints201907.0102.v1

Table 2. List of microglia cell proteins identified in the three representative clusters after ANOVA with a Statistical analysis with p value = 0.05.

Cluster 1		Cluster 2		Cluster 3			
Gene name	Protein name	Gene name	Protein name	Gene name	Protein name	Gene name	Protein name
Gnb4	G Protein Subunit Beta 4	Slc7a2	Solute Carrier Family 7 Member 2	Drap 1	DR1 Associated Protein 1	Hist1 h2ba	Histone Cluster 1 H2B Family Member A
Fdft1	Farnesyl-Diphosphate Farnesyltransferase 1	Ltbp2	Latent Transforming Growth Factor Beta Binding Protein 2	Capz a1	Capping Actin Protein of Muscle Z-Line Alpha Subunit 1	Gfm1	G Elongation Factor Mitochondrial 1
Goli m4	Golgi Integral Membrane Protein 4	Serpinb 2	Serpin Family B Member 2	Pgp	Phosphoglycolate Phosphatase	Lpcat 1	Lysophosphatidylcholine Acyltransferase 1
Gsn	Gelsolin	Lcn2	Lipocalin 2	Hist1 h1a	Histone Cluster 1 H1 Family Member A	Ppp2r 1b	Protein Phosphatase 2 Scaffold Subunit Abeta
Uqcrc 1	Ubiquinol-Cytochrome C Reductase Core Protein I	Thbs4	Thrombospondin 4	C1qb p	Complement C1q Binding Protein	Mat2 b	Methionine Adenosyltransferase 2B
Pde12	Phosphodiesterase 12	Atp7a	ATPase Copper Transporting Alpha	Hprt1	Hypoxanthine Phosphoribosyltransferase 1	Nudt 9	Nudix Hydrolase 9
Naa35	N(Alpha)-Acetyltransferase 35, NatC Auxiliary Subunit	Nos2	Nitric Oxide Synthase 2	Ssbp1	Single Stranded DNA Binding Protein 1	Pelo	Pelota MRNA Surveillance and Ribosome Rescue Factor
Faf1	Fas Associated Factor 1	Cog7	Component of Oligomeric Golgi Complex 7	Psmb 6	Proteasome Subunit Beta 6	Unc1 19	Unc-119 Lipid Binding Chaperone
Clip1	CAP-Gly Domain Containing Linker Protein 1			Pggt1 b	Protein Geranylgeranyltransferase Type I Subunit Beta	Eif2b 4	Eukaryotic Translation Initiation Factor 2B Subunit Delta
				Nutf2	Nuclear Transport Factor 2	Far1	Fatty Acyl-CoA Reductase 1
				Phb	Prohibitin	Dek	DEK Proto-Oncogene
				Tubg 1	Tubulin Gamma 1	Rab21	RAB21, Member RAS Oncogene Family
				Tceb1	Elongin C	Dhrs4	Dehydrogenase/ Reductase 4
				Bpnt1	3'(2'),5'-Bisphosphate Nucleotidase 1	Synpo	Synaptopodin

Preprints (www.preprints.org) | NOT PEER-REVIEWED | Posted: 8 July 2019 doi:10.20944/preprints201907.0102.v1

Table 3. LFQ value of the identified proteins involved in immune response or neurogenesis from microglia issued from two different territories (cortex or spinal cord).

T: Gene names	T: Protein names	cortex_control	cortex_LPS	Spinal_cord_control	Spinal_cord_LPS
Cd14	Monocyte differentiation antigen CD14	28,0689	30,6709	27,7018	30,3253
Cd151	CD151 antigen	26,7143	26,5756	27,9371	27,2832
Cd1d	Antigen-presenting glycoprotein CD1d	27,0964	26,3685	27,075	26,4533
Cd200	OX-2 membrane glycoprotein	NaN	NaN	NaN	26,359
Cd36	Platelet glycoprotein 4	26,6613	25,9943	NaN	24,1633
Cd38	ADP-ribosyl cyclase/cyclic ADP-ribose hydrolase 1	25,4339	25,6477	NaN	NaN
Cd4	T-cell surface glycoprotein CD4	24,9021	25,0884	NaN	NaN
Cd44	CD44 antigen	28,6762	30,1132	28,7624	30,0004
Cd47	Leukocyte surface antigen CD47	26,8879	27,4734	27,897	28,5647
Cd48	CD48 antigen	26,8801	27,0697	NaN	26,5038
Cd59	CD59 glycoprotein	NaN	NaN	NaN	24,0947
Cd63	CD63 antigen	25,8967	26,345	NaN	26,4007
Cd81	CD81 antigen	26,6434	26,3571	25,7896	26,035
Cd82	CD82 antigen	NaN	27,683	NaN	27,9846
Lgals1	Galectin-1	31,5512	31,1253	30,5223	30,2404
Lgals3	Galectin-3	25,7619	27,7496	NaN	26,5787
Lgals3bp	Galectin-3-binding protein	25,7619	27,7496	NaN	26,5787
Lgals9	Galectin-9	25,831	26,4202	25,6608	25,8864
Irf2bpl	Interferon regulatory factor 2-binding protein-like	23,6893	24,0285	NaN	NaN
Mx1	Interferon-induced GTP-binding protein Mx1	27,1942	32,6644	26,7569	32,8196
Mx2	Interferon-induced GTP-binding protein Mx2	NaN	NaN	NaN	28,8021
Mx3	Interferon-induced GTP-binding protein Mx3	27,326	32,4824	27,0963	32,3658
Gbp2	Interferon-induced guanylate-binding protein 2	28,6871	30,4046	27,475	29,9928
ifitm3	Interferon-induced transmembrane protein 3	29,9927	29,014	28,3237	29,2098
Eif2ak2	Interferon-induced, double-stranded RNA-activated protein kinase	27,3957	28,2147	26,4888	27,3009
Prkra	Interferon-inducible double-stranded RNA-dependent protein kinas	27,2149	27,4385	NaN	27,2515
Ilf2	Interleukin enhancer-binding factor 2	27,1955	27,4402	27,1603	27,2551
Ilf3	Interleukin enhancer-binding factor 3	28,8886	28,698	27,8844	29,1216
Il1b	Interleukin-1 beta	28,463	29,6775	NaN	30,334
Il1rn	Interleukin-1 receptor antagonist protein	26,9663	28,0446	27,6581	29,1706
Il18	Interleukin-18	NaN	26,0856	NaN	NaN
Nlrc4	NLR family CARD domain-containing protein 4	NaN	25,6347	NaN	NaN
Casp1	Caspase-1;Caspase-1 subunit p20;Caspase-1 subunit p10	26,3379	26,9017	26,1236	26,4076
Casp3	Caspase-3;Caspase-3 subunit p17;Caspase-3 subunit p12	25,9244	25,9588	NaN	25,6891
Casp6	Caspase-6;Caspase-6 subunit p18;Caspase-6 subunit p11	24,7235	24,7551	NaN	NaN
Casp8	Caspase-8;Caspase-8 subunit p18;Caspase-8 subunit p10	25,1924	25,8941	25,4846	26,3666
Fcgrt	IgG receptor FcRn large subunit p51	26,8531	26,4137	26,8162	26,1217
Fcgr2	Low affinity immunoglobulin gamma Fc region receptor II	26,6778	27,5849	25,6272	26,9442
Fcgr3	Low affinity immunoglobulin gamma Fc region receptor III	27,332	28,9923	NaN	26,3924
Tgfb1i1	Transforming growth factor beta-1-induced transcript 1 protein	27,6412	27,6039	27,3103	26,9776
Ccl7	C-C motif chemokine 7	NaN	27,5368	NaN	28,5752
C3	Complement C3;Complement C3 beta chain;C3-beta-c;Complement C	27,1688	28,6963	NaN	28,1336
C5ar1	C5a anaphylatoxin chemotactic receptor 1	28,59	29,1114	NaN	NaN
B2m	Beta-2-microglobulin	26,6971	28,8647	NaN	NaN
RT1-Aw2	Class I histocompatibility antigen, Non-RT1.A alpha-1 chain	26,3063	28,5597	27,1941	28,3661
Spg21	Maspardin	28,0336	27,8525	27,7823	27,7344
Lyz1;Lyz2	Lysozyme C-1;Putative lysozyme C-2	30,1086	30,3596	26,7459	28,1551
Serpinb1a	Leukocyte elastase inhibitor A	29,9389	29,4702	29,4359	29,2674
Cd47	Leukocyte surface antigen CD47	26,8879	27,4734	27,897	28,5647
Lta4h	Leukotriene A-4 hydrolase	30,5007	30,413	29,7105	29,5928
Mif	Macrophage migration inhibitory factor	27,7384	27,9528	27,2929	27,7102
Capg	Macrophage-capping protein	33,5188	33,7409	32,8733	32,9981
Mpeg1	Macrophage-expressed gene 1 protein	25,8386	26,9181	24,9908	27,5517
A1m	Alpha-1-macroglobulin;Alpha-1-macroglobulin 45 kDa subunit	26,6489	24,6148	NaN	27,0497
Lrpap1	Alpha-2-macroglobulin receptor-associated protein	29,1395	29,1856	30,2142	28,7722
Nenf	Neudesin	26,0403	26,344	26,3001	25,8054
Ostf1	Osteoclast-stimulating factor 1	29,5709	29,528	30,0009	30,0559
Spp1	Osteopontin	NaN	24,7234	NaN	NaN
Plec	Plectin	31,0691	29,7337	27,6853	31,1381
Ndrg1	Protein NDRG1	27,9087	27,6558	27,9143	27,9117

Preprints (www.preprints.org) | NOT PEER-REVIEWED | Posted: 8 July 2019 doi:10.20944/preprints201907.0102.v1

Appendix A.2: Figures

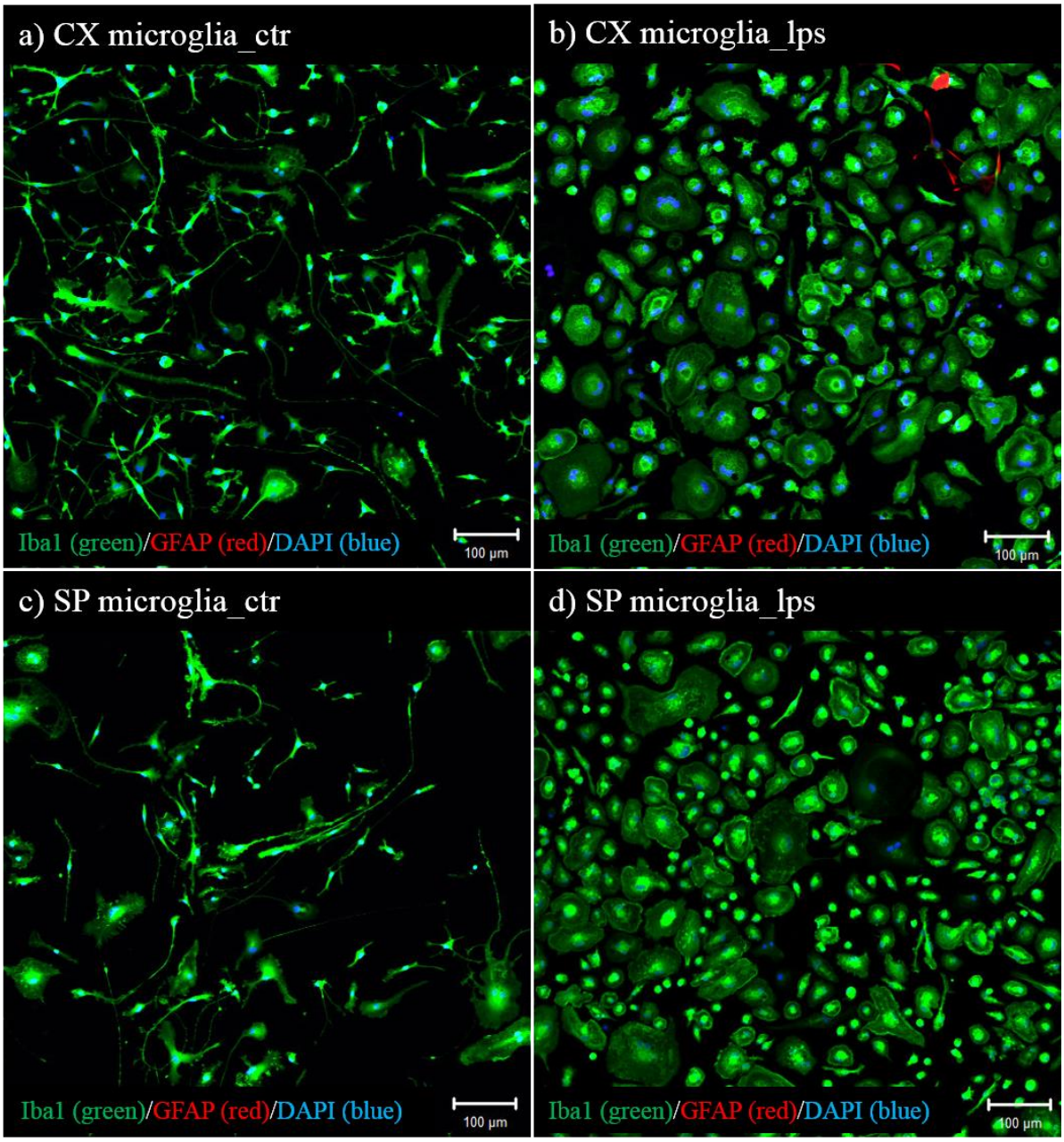

Figure 1. Morphological changes of microglia after LPS stimulation. (A) Cortex microglia non-treated (control) and (B) treated with 500ng/mL LPS for 24h. (C) Spinal cord microglia non-treated (control) and (D) treated with 500ng/mL LPS for 24h. Immunostaining using anti-Iba1 antibody (green), marker for microglia cells, anti-GFAP antibody (red), marker for astrocytes and DAPI (blue) stain for cell nucleus. Scale bars: 100 µm.

Preprints (www.preprints.org) | NOT PEER-REVIEWED | Posted: 8 July 2019 doi:10.20944/preprints201907.0102.v1

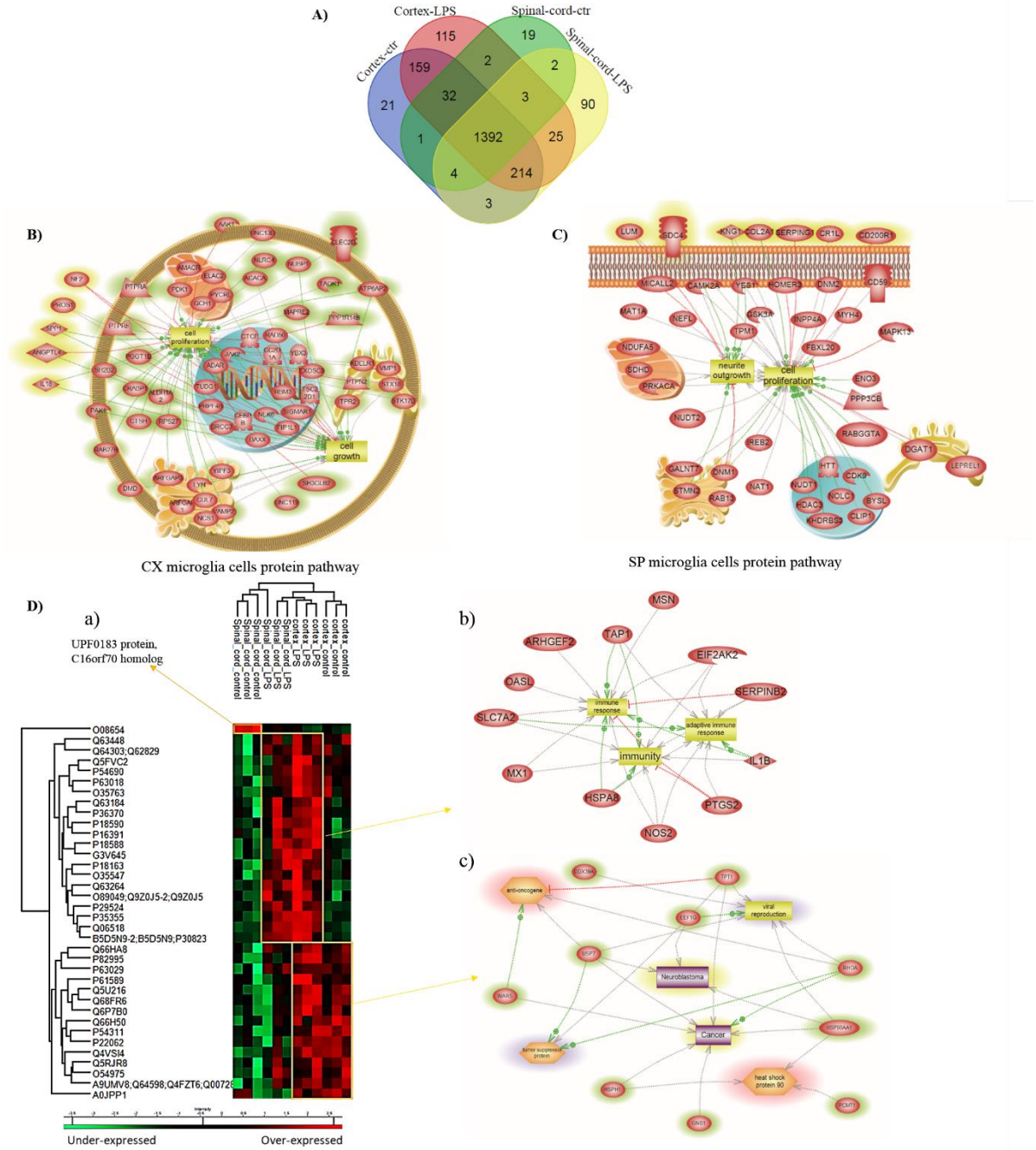

Figure 2. Shot gun analyses of proteins isolated from cortex or spinal cord microglia. (A) Venn diagram of the unique protein of microglia cells. Pathway analyses of specific proteins isolated from (B) cortex after LPS treatment 500ng/mL LPS for 24h, (C) spinal cord control, and (D) spinal cord treated with 500ng/mL LPS for 24h . Representative Heat map a) of the common proteins and quantified by label free and analyses by MaxQuant with a P value =0.05 and pathways obtained from each cluster b) pathway analyses of cluster 2 common to spinal cord and cortex microglia after LPS treatment and c) Pathway analyses of cluster 3 containing only cortex microglia. The analyses were performed in triplicate (n=3).

Preprints (www.preprints.org) | NOT PEER-REVIEWED | Posted: 8 July 2019 doi:10.20944/preprints201907.0102.v1

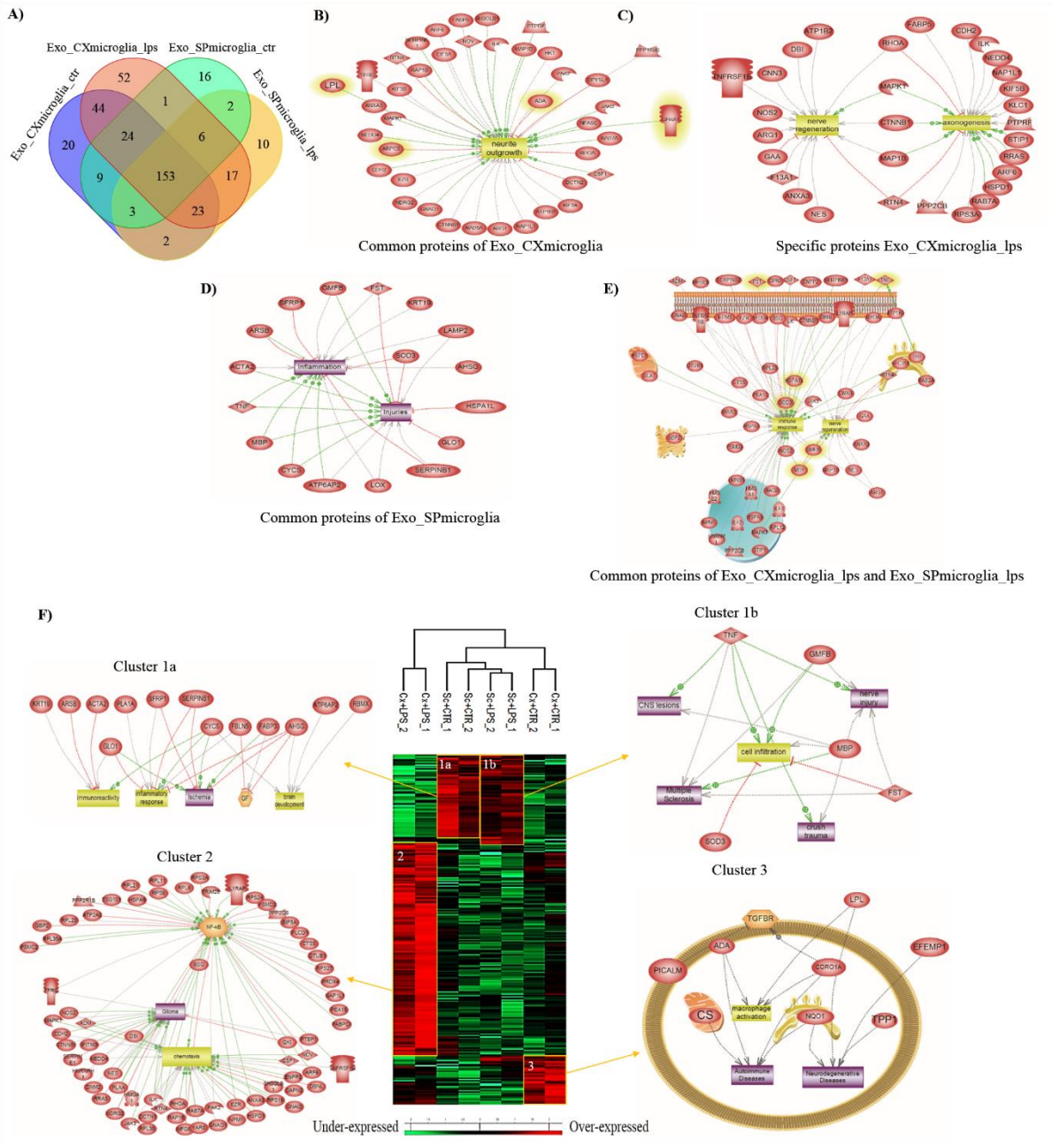

Figure 3. Systemic biology analysis of proteins identified by Shot-gun proteomic derived from microglia exosomes. (A) Venn diagram of proteins of exosomes released by microglia. Pathway analyses of (B) common protein from exosomes of cortex microglia treated or not with 500ng/mL LPS for 24h (C) specific proteins from exosomes of cortex microglial cells treated with 500ng/mL LPS for 24h (D) common protein from exosomes of spinal cord microglia treated or not with 500ng/mL LPS for 24h and (E) common protein of exosomes released cortex and spinal cord microglia treated with LPS. (F) Heatmap from shot proteomic analysis using MaxQuant after ANOVA with a p value >0.05 for exosomes released by microglia isolated from two different sources, cortex and spinal cord, and pathways issued from systemic biology analyses of cluster 1, 2 and 3 from the heatmap. The analyses were performed in replicate (n=3).

Preprints (www.preprints.org) | NOT PEER-REVIEWED | Posted: 8 July 2019 doi:10.20944/preprints201907.0102.v1

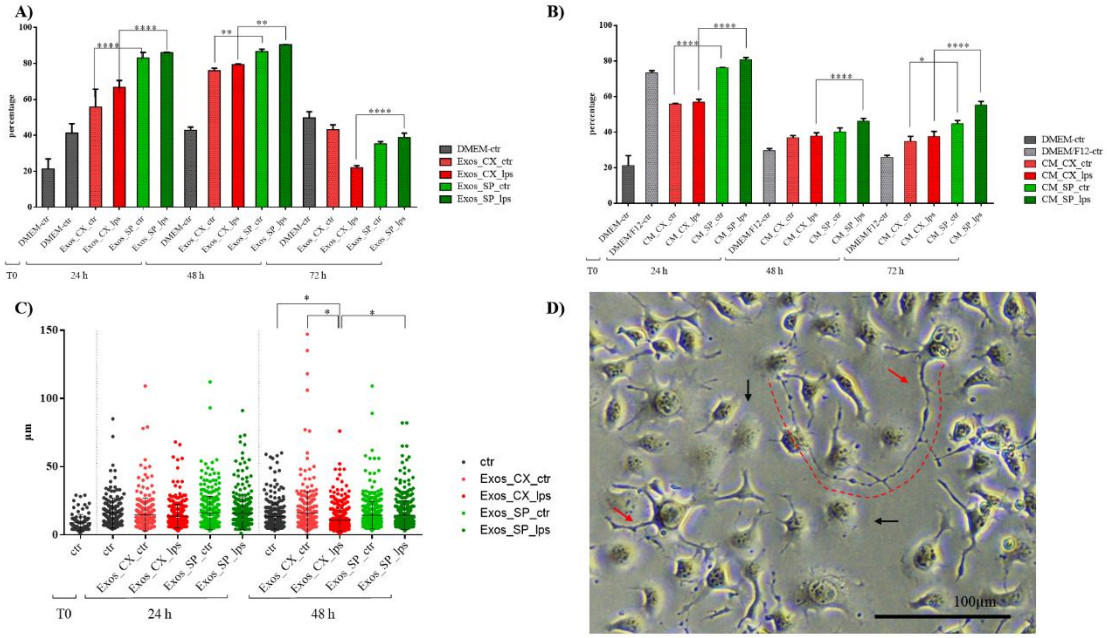

Figure 4. Microglia-derived exosomes and conditioned medium modulate neurites outgrowth in DRG cells line (ND7/23). (A) Time course (24h - 72h) analyses were performed with exosomes, (B) or with microglia's conditioned medium depleted of exosomes and correlated to the number of neurites per cells that emerged (percentage). (C) Box plot representation of a time course (24h, 48h) of the neurite lengths growth after treatment with exosomes (equal quantity for each group of cells – 1.5E+08particles). (D) Explicit image of DRGs cells neurites outgrowth after treatment with microglia exosomes. Red arrows indicate DRGs neurites that occurred after incubation with microglia exosomes. Scale bars: 100 µm.

Preprints (www.preprints.org) | NOT PEER-REVIEWED | Posted: 8 July 2019 doi:10.20944/preprints201907.0102.v1

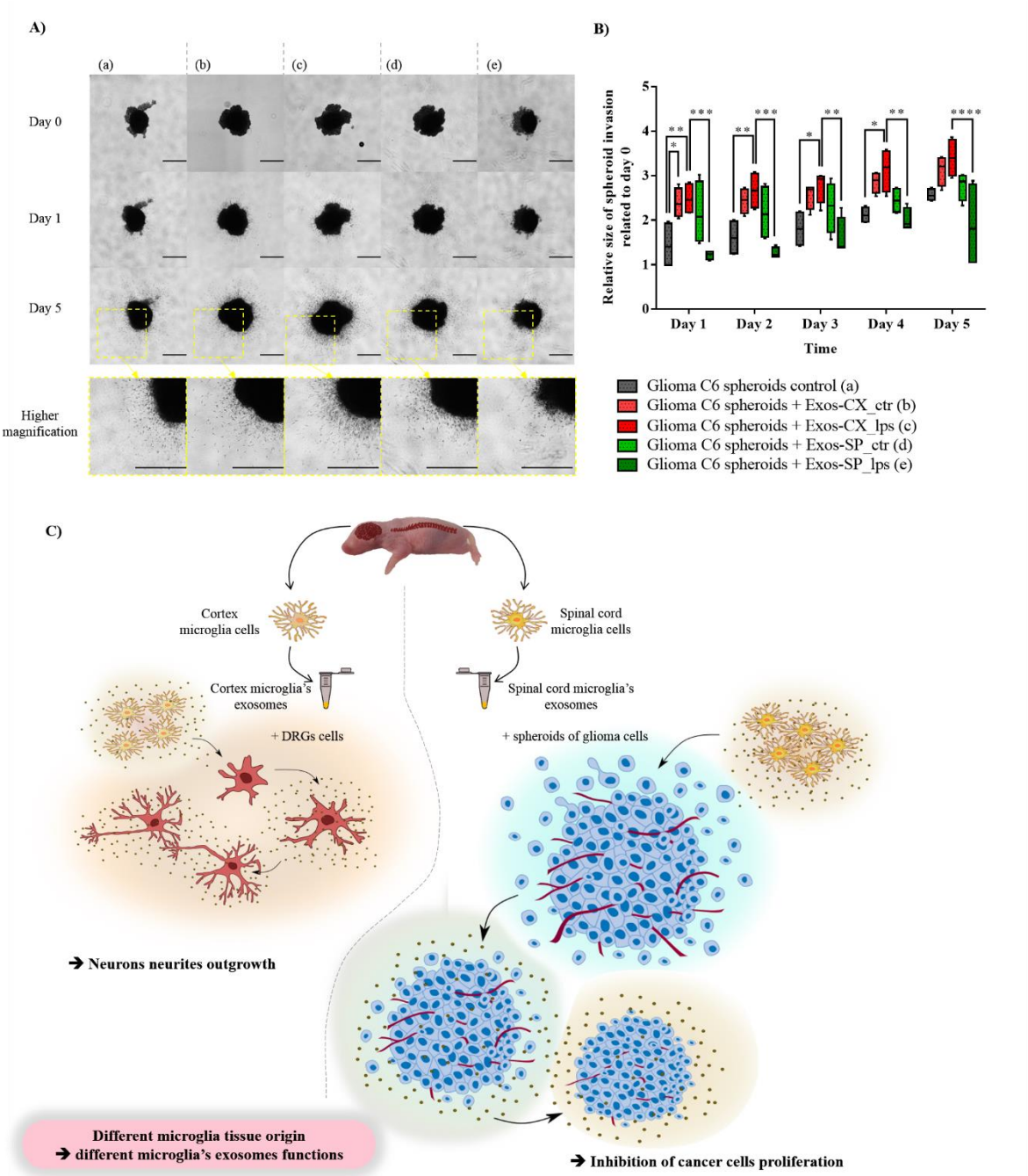

Figure 5. Impact of microglia derived exosomes on glioma spheroids. (A) Representative images of the invasion of C6 spheroids in the collagen matrix at day 0, 1 and 5. Spheroids are in the absence or in the presence of exosomes released by microglia cells (cortex or spinal cord) not treated or treated with 500ng/mL LPS for 24h. All images were acquired with an inverted light microscope at 5x magnification. Scale bar: 500 µm. Inset represent spheroid at day 5 at a higher magnification. The results obtained are depicted through a box plot figure. Significant differences were identified using Tukey's multiple comparisons test. (C) **General summary.** The scheme represents the impact on biological function i.e. neurites outgrowth or glioma proliferation inhibition of microglia derived exosomes upon their original localization (cortex or spinal cord).

Preprints (www.preprints.org) | NOT PEER-REVIEWED | Posted: 8 July 2019 doi:10.20944/preprints201907.0102.v1

References

1. Chan, W.Y.; Kohsaka, S.; Rezaie, P. The origin and cell lineage of microglia—New concepts. *Brain Research Reviews* **2007**, *53*, 344–354.
2. Conde, J.R.; Streit, W.J. Microglia in the aging brain. *J. Neuropathol. Exp. Neurol.* **2006**, *65*, 199–203.
3. Prinz, M.; Erny, D.; Hagemeyer, N. Ontogeny and homeostasis of CNS myeloid cells. *Nature Immunology* **2017**, *18*, 385–392.
4. Bennett, M.L.; Bennett, F.C.; Liddelow, S.A.; Ajami, B.; Zamanian, J.L.; Fernhoff, N.B.; Mulinyawe, S.B.; Bohlen, C.J.; Adil, A.; Tucker, A.; et al. New tools for studying microglia in the mouse and human CNS. *Proc. Natl. Acad. Sci. U.S.A.* **2016**, *113*, E1738-1746.
5. Ginhoux, F.; Greter, M.; Leboeuf, M.; Nandi, S.; See, P.; Gokhan, S.; Mehler, M.F.; Conway, S.J.; Ng, L.G.; Stanley, E.R.; et al. Fate mapping analysis reveals that adult microglia derive from primitive macrophages. *Science* **2010**, *330*, 841–845.
6. Hoeffel, G.; Ginhoux, F. Ontogeny of Tissue-Resident Macrophages. *Front Immunol* **2015**, *6*, 486.
7. Tay, T.L.; Hagemeyer, N.; Prinz, M. The force awakens: insights into the origin and formation of microglia. *Curr. Opin. Neurobiol.* **2016**, *39*, 30–37.
8. Dalmau, I.; Vela, J.M.; González, B.; Finsen, B.; Castellano, B. Dynamics of microglia in the developing rat brain. *J. Comp. Neurol.* **2003**, *458*, 144–157.
9. Hagemeyer, N.; Hanft, K.-M.; Akriditou, M.-A.; Unger, N.; Park, E.S.; Stanley, E.R.; Staszewski, O.; Dimou, L.; Prinz, M. Microglia contribute to normal myelinogenesis and to oligodendrocyte progenitor maintenance during adulthood. *Acta Neuropathol.* **2017**, *134*, 441–458.
10. Michell-Robinson, M.A.; Touil, H.; Healy, L.M.; Owen, D.R.; Durafourt, B.A.; Bar-Or, A.; Antel, J.P.; Moore, C.S. Roles of microglia in brain development, tissue maintenance and repair. *Brain* **2015**, *138*, 1138–1159.
11. Safaiyan, S.; Kannaiyan, N.; Snaidero, N.; Brioschi, S.; Biber, K.; Yona, S.; Edinger, A.L.; Jung, S.; Rossner, M.J.; Simons, M. Age-related myelin degradation burdens the clearance function of microglia during aging. *Nat. Neurosci.* **2016**, *19*, 995–998.
12. Sheffield, L.G.; Berman, N.E. Microglial expression of MHC class II increases in normal aging of nonhuman primates. *Neurobiol. Aging* **1998**, *19*, 47–55.
13. Streit, W.J. Microglia as neuroprotective, immunocompetent cells of the CNS. *Glia* **2002**, *40*, 133–139.
14. Varol, D.; Mildner, A.; Blank, T.; Shemer, A.; Barashi, N.; Yona, S.; David, E.; Boura-Halfon, S.; Segal-Hayoun, Y.; Chappell-Maor, L.; et al. Dicer Deficiency Differentially Impacts Microglia of the Developing and Adult Brain. *Immunity* **2017**, *46*, 1030-1044.e8.
15. Wlodarczyk, A.; Holtman, I.R.; Krueger, M.; Yogev, N.; Bruttger, J.; Khorooshi, R.; Benmamar-Badel, A.; de Boer-Bergsma, J.J.; Martin, N.A.; Karram, K.; et al. A novel microglial subset plays a key role in myelinogenesis in developing brain. *EMBO J.* **2017**, *36*, 3292–3308.
16. Frost, J.L.; Schafer, D.P. Microglia: Architects of the Developing Nervous System. *Trends Cell Biol.* **2016**, *26*, 587–597.
17. Perez-Pouchoulen, M.; VanRyzin, J.W.; McCarthy, M.M. Morphological and Phagocytic Profile of Microglia in the Developing Rat Cerebellum. *eNeuro* **2015**, *2*, ENEURO.0036-15.2015.
18. Ginhoux, F.; Guilliams, M. Tissue-Resident Macrophage Ontogeny and Homeostasis. *Immunity* **2016**, *44*, 439–449.
19. Ginhoux, F.; Merad, M. [Microglia arise from extra-embryonic yolk sac primitive progenitors]. *Med Sci (Paris)* **2011**, *27*, 719–724.
20. Greter, M.; Merad, M. Regulation of microglia development and homeostasis. *Glia* **2013**, *61*, 121–127.
21. Lavin, Y.; Mortha, A.; Rahman, A.; Merad, M. Regulation of macrophage development and function in peripheral tissues. *Nat. Rev. Immunol.* **2015**, *15*, 731–744.
22. Lavin, Y.; Winter, D.; Blecher-Gonen, R.; David, E.; Keren-Shaul, H.; Merad, M.; Jung, S.; Amit, I. Tissue-resident macrophage enhancer landscapes are shaped by the local microenvironment. *Cell* **2014**, *159*, 1312–1326.
23. Yamasaki, R.; Lu, H.; Butovsky, O.; Ohno, N.; Rietsch, A.M.; Cialic, R.; Wu, P.M.; Doykan, C.E.; Lin, J.; Cotleur, A.C.; et al. Differential roles of microglia and monocytes in the inflamed central nervous system. *J. Exp. Med.* **2014**, *211*, 1533–1549.

Preprints (www.preprints.org) | NOT PEER-REVIEWED | Posted: 8 July 2019 doi:10.20944/preprints201907.0102.v1

24. Schulz, C.; Gomez Perdiguero, E.; Chorro, L.; Szabo-Rogers, H.; Cagnard, N.; Kierdorf, K.; Prinz, M.; Wu, B.; Jacobsen, S.E.W.; Pollard, J.W.; et al. A lineage of myeloid cells independent of Myb and hematopoietic stem cells. *Science* **2012**, *336*, 86–90.
25. Butovsky, O.; Jedrychowski, M.P.; Moore, C.S.; Cialic, R.; Lanser, A.J.; Gabriely, G.; Koeglsperger, T.; Dake, B.; Wu, P.M.; Doykan, C.E.; et al. Identification of a unique TGF-β-dependent molecular and functional signature in microglia. *Nat. Neurosci.* **2014**, *17*, 131–143.
26. Théry, C. Exosomes: secreted vesicles and intercellular communications. *F1000 Biol Rep* **2011**, *3*.
27. Choi, D.-S.; Kim, D.-K.; Kim, Y.-K.; Gho, Y.S. Proteomics of extracellular vesicles: Exosomes and ectosomes. *Mass Spec Rev* **2015**, *34*, 474–490.
28. Brites, D.; Fernandes, A. Neuroinflammation and Depression: Microglia Activation, Extracellular Microvesicles and microRNA Dysregulation. *Front Cell Neurosci* **2015**, *9*, 476.
29. Norden, D.M.; Godbout, J.P. Review: microglia of the aged brain: primed to be activated and resistant to regulation. *Neuropathol. Appl. Neurobiol.* **2013**, *39*, 19–34.
30. Perry, V.H.; Holmes, C. Microglial priming in neurodegenerative disease. *Nat Rev Neurol* **2014**, *10*, 217–224.
31. Matcovitch-Natan, O.; Winter, D.R.; Giladi, A.; Aguilar, S.V.; Spinrad, A.; Sarrazin, S.; Ben-Yehuda, H.; David, E.; González, F.Z.; Perrin, P.; et al. Microglia development follows a stepwise program to regulate brain homeostasis. *Science* **2016**, aad8670.
32. Thion, M.S.; Low, D.; Silvin, A.; Chen, J.; Grisel, P.; Schulte-Schrepping, J.; Blecher, R.; Ulas, T.; Squarzoni, P.; Hoeffel, G.; et al. Microbiome Influences Prenatal and Adult Microglia in a Sex-Specific Manner. *Cell* **2018**, *172*, 500-516.e16.
33. Silvin, A.; Ginhoux, F. Microglia heterogeneity along a spatio–temporal axis: More questions than answers. *Glia* **2018**, *66*, 2045–2057.
34. Haas, A.H. de; Boddeke, H.W.G.M.; Biber, K. Region-specific expression of immunoregulatory proteins on microglia in the healthy CNS. *Glia* **2008**, *56*, 888–894.
35. Scheffel, J.; Regen, T.; Rossum, D.V.; Seifert, S.; Ribes, S.; Nau, R.; Parsa, R.; Harris, R.A.; Boddeke, H.W.G.M.; Chuang, H.-N.; et al. Toll-like receptor activation reveals developmental reorganization and unmasks responder subsets of microglia. *Glia* **2012**, *60*, 1930–1943.
36. Murgoci, A.-N.; Cizkova, D.; Majerova, P.; Petrovova, E.; Medvecky, L.; Fournier, I.; Salzet, M. Brain-Cortex Microglia-Derived Exosomes: Nanoparticles for Glioma Therapy. *Chemphyschem* **2018**.
37. Cisneros Castillo, L.R.; Oancea, A.-D.; Stüllein, C.; Régnier-Vigouroux, A. Evaluation of Consistency in Spheroid Invasion Assays. *Sci Rep* **2016**, *6*.
38. Duhamel, M.; Rose, M.; Rodet, F.; Murgoci, A.-N.; Zografidou, L.; Régnier-Vigouroux, A.; Vanden Abeele, F.; Kobeissy, F.; Nataf, S.; Pays, L.; et al. Paclitaxel treatment and PC1/3 knockdown in macrophages is a promising anti-glioma strategy as revealed by proteomics and cytotoxicity studies. *Mol. Cell Proteomics* **2018**.
39. Wiśniewski, J.R.; Zougman, A.; Nagaraj, N.; Mann, M. Universal sample preparation method for proteome analysis. *Nat. Methods* **2009**, *6*, 359–362.
40. Cox, J.; Mann, M. MaxQuant enables high peptide identification rates, individualized p.p.b.-range mass accuracies and proteome-wide protein quantification. *Nat. Biotechnol.* **2008**, *26*, 1367–1372.
41. Cox, J.; Neuhauser, N.; Michalski, A.; Scheltema, R.A.; Olsen, J.V.; Mann, M. Andromeda: a peptide search engine integrated into the MaxQuant environment. *J. Proteome Res.* **2011**, *10*, 1794–1805.
42. UniProt Consortium Reorganizing the protein space at the Universal Protein Resource (UniProt). *Nucleic Acids Res.* **2012**, *40*, D71-75.
43. Lago, N.; Pannunzio, B.; Amo-Aparicio, J.; López-Vales, R.; Peluffo, H. CD200 modulates spinal cord injury neuroinflammation and outcome through CD200R1. *Brain Behav. Immun.* **2018**.
44. Rogall, R.; Pikhovych, A.; Bach, A.; Hoehn, M.; Couillard-Despres, S.; Fink, G.R.; Schroeter, M.; Rueger, M.A. P 4 Bioluminescence imaging visualizes osteopontin-induced neurogenesis and neuroblasts migration in the mouse brain after stroke. *Clinical Neurophysiology* **2017**, *128*, e327–e328.
45. Kim, D.-K.; Kang, B.; Kim, O.Y.; Choi, D.; Lee, J.; Kim, S.R.; Go, G.; Yoon, Y.J.; Kim, J.H.; Jang, S.C.; et al. EVpedia: an integrated database of high-throughput data for systemic analyses of extracellular vesicles. *Journal of Extracellular Vesicles* **2013**, *2*.
46. Cizkova, D.; Le Marrec-Croq, F.; Franck, J.; Slovinska, L.; Grulova, I.; Devaux, S.; Lefebvre, C.; Fournier, I.; Salzet, M. Alterations of protein composition along the rostro-caudal axis after spinal cord injury: proteomic, in vitro and in vivo analyses. *Front Cell Neurosci* **2014**, *8*, 105.

Preprints (www.preprints.org) | NOT PEER-REVIEWED | Posted: 8 July 2019 doi:10.20944/preprints201907.0102.v1

47. Devaux, S.; Cizkova, D.; Quanico, J.; Franck, J.; Nataf, S.; Pays, L.; Hauberg-Lotte, L.; Maass, P.; Kobarg, J.H.; Kobeissy, F.; et al. Proteomic Analysis of the Spatio-temporal Based Molecular Kinetics of Acute Spinal Cord Injury Identifies a Time- and Segment-specific Window for Effective Tissue Repair. *Mol. Cell Proteomics* **2016**, *15*, 2641–2670.
48. Devaux, S.; Cizkova, D.; Mallah, K.; Karnoub, M.A.; Laouby, Z.; Kobeissy, F.; Blasko, J.; Nataf, S.; Pays, L.; Mériaux, C.; et al. RhoA Inhibitor Treatment At Acute Phase of Spinal Cord Injury May Induce Neurite Outgrowth and Synaptogenesis. *Mol. Cell Proteomics* **2017**, *16*, 1394–1415.
49. Ginhoux, F.; Prinz, M. Origin of Microglia: Current Concepts and Past Controversies. *Cold Spring Harbor Perspectives in Biology* **2015**, *7*, a020537.
50. Li, Q.; Barres, B.A. Microglia and macrophages in brain homeostasis and disease. *Nat. Rev. Immunol.* **2018**, *18*, 225–242.
51. Askew, K.; Li, K.; Olmos-Alonso, A.; Garcia-Moreno, F.; Liang, Y.; Richardson, P.; Tipton, T.; Chapman, M.A.; Riecken, K.; Beccari, S.; et al. Coupled Proliferation and Apoptosis Maintain the Rapid Turnover of Microglia in the Adult Brain. *Cell Rep* **2017**, *18*, 391–405.
52. Böttcher, C.; Schlickeiser, S.; Sneeboer, M.A.M.; Kunkel, D.; Knop, A.; Paza, E.; Fidzinski, P.; Kraus, L.; Snijders, G.J.L.; Kahn, R.S.; et al. Human microglia regional heterogeneity and phenotypes determined by multiplexed single-cell mass cytometry. *Nat. Neurosci.* **2019**, *22*, 78–90.
53. Frakes, A.E.; Ferraiuolo, L.; Haidet-Phillips, A.M.; Schmelzer, L.; Braun, L.; Miranda, C.J.; Ladner, K.J.; Bevan, A.K.; Foust, K.D.; Godbout, J.P.; et al. Microglia induce motor neuron death via the classical NF-κB pathway in amyotrophic lateral sclerosis. *Neuron* **2014**, *81*, 1009–1023.
54. Nikodemova, M.; Small, A.L.; Smith, S.M.C.; Mitchell, G.S.; Watters, J.J. Spinal but not cortical microglia acquire an atypical phenotype with high VEGF, galectin-3 and osteopontin, and blunted inflammatory responses in ALS rats. *Neurobiol. Dis.* **2014**, *69*, 43–53.
55. Ginhoux, F.; Lim, S.; Hoeffel, G.; Low, D.; Huber, T. Origin and differentiation of microglia. *Front Cell Neurosci* **2013**, *7*, 45.
56. Grabert, K.; Michoel, T.; Karavolos, M.H.; Clohisey, S.; Baillie, J.K.; Stevens, M.P.; Freeman, T.C.; Summers, K.M.; McColl, B.W. Microglial brain region-dependent diversity and selective regional sensitivities to aging. *Nat. Neurosci.* **2016**, *19*, 504–516.
57. Edman, L.C.; Mira, H.; Arenas, E. The beta-chemokines CCL2 and CCL7 are two novel differentiation factors for midbrain dopaminergic precursors and neurons. *Exp. Cell Res.* **2008**, *314*, 2123–2130.
58. Jones, E.V.; Bouvier, D.S. Astrocyte-secreted matricellular proteins in CNS remodelling during development and disease. *Neural Plast.* **2014**, *2014*, 321209.
59. Malik, A.R.; Liszewska, E.; Jaworski, J. Matricellular proteins of the Cyr61/CTGF/NOV (CCN) family and the nervous system. *Front Cell Neurosci* **2015**, *9*, 237.
60. Norden, D.M.; Faw, T.D.; McKim, D.B.; Deibert, R.J.; Fisher, L.C.; Sheridan, J.F.; Godbout, J.P.; Basso, D.M. Bone Marrow-Derived Monocytes Drive the Inflammatory Microenvironment in Local and Remote Regions after Thoracic Spinal Cord Injury. *J. Neurotrauma* **2018**.
61. Huang, S.; Ge, X.; Yu, J.; Han, Z.; Yin, Z.; Li, Y.; Chen, F.; Wang, H.; Zhang, J.; Lei, P. Increased miR-124-3p in microglial exosomes following traumatic brain injury inhibits neuronal inflammation and contributes to neurite outgrowth via their transfer into neurons. *The FASEB Journal* **2017**, *32*, 512–528.
62. Paolicelli, R.C.; Bergamini, G.; Rajendran, L. Cell-to-cell Communication by Extracellular Vesicles: Focus on Microglia. *Neuroscience* **2018**.
63. Gayle, D.; Ilyin, S.E.; Miele, M.E.; Plata-Salamán, C.R. Modulation of TNF-alpha mRNA production in rat C6 glioma cells by TNF-alpha, IL-1beta, IL-6, and IFN-alpha: in vitro analysis of cytokine-cytokine interactions. *Brain Res. Bull.* **1998**, *47*, 231–235.
64. Wang, M.; Wang, T.; Liu, S.; Yoshida, D.; Teramoto, A. The expression of matrix metalloproteinase-2 and -9 in human gliomas of different pathological grades. *Brain Tumor Pathol* **2003**, *20*, 65–72.
65. Framson, P.E.; Sage, E.H. SPARC and tumor growth: where the seed meets the soil? *J. Cell. Biochem.* **2004**, *92*, 679–690.